JACS
JOURNAL OF THE AMERICAN CHEMICAL SOCIETY
Article
pubs.acs.org/JACS

Transition-Metal-Free CO-Releasing BODIPY Derivatives Activatable by Visible to NIR Light as Promising Bioactive Molecules

Eduardo Palao,[†,∥] Tomáš Slanina,[†,∥] Lucie Muchová,[‡] Tomáš Šolomek,[†] Libor Vítek,[‡,§] and Petr Klán*[,†]

[†]Department of Chemistry and RECETOX, Masaryk University, Kamenice 5, 625 00 Brno, Czech Republic
[‡]Institute of Medical Biochemistry and Laboratory Diagnostics, 1st Faculty of Medicine, and [§]4th Department of Internal Medicine, 1st Faculty of Medicine, Charles University in Prague, Na Bojišti 3, 121 08 Praha 2, Czech Republic

Supporting Information

ABSTRACT: Carbon monoxide-releasing molecules (CORMs) are chemical agents used to administer CO as an endogenous, biologically active molecule. A precise spatial and temporal control over the CO release is the major requirement for their applications. Here, we report the synthesis and properties of a new generation of transition-metal-free carbon monoxide-releasing molecules based on BODIPY chromophores (COR-BDPs) activatable by visible-to-NIR (up to 730 nm) light. We demonstrate their performance for both in vitro and in vivo experimental settings, and we propose the mechanism of the CO release based on steady-state and transient spectroscopy experiments and quantum chemical calculations.

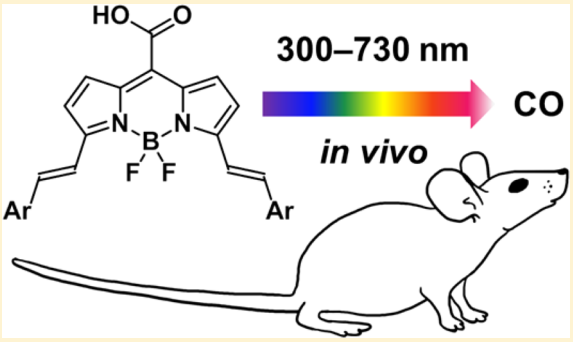

INTRODUCTION

Carbon monoxide is known for its lethal effects in mammals because it binds to hemoglobin more strongly than oxygen.[1] However, it is now evident that CO is an important cell-signaling molecule with substantial therapeutic potential protecting from vascular, inflammatory, or even cancer diseases.[2−6]

Carbon monoxide-releasing molecules (CORMs) have been developed to deliver CO into the cell.[3,7−11] The most important criteria for designing CORMs are chemical stability when stored as well as aqueous solubility, temporal control over the CO release, and low toxicity in their in vivo applications. Unlike other signaling molecules, such as NO or H_2S, CO is a stable and inert molecule that reacts only with transition metals.[1] Thus, with a few exceptions, such as boranocarbonates[12] or an interesting "click and release" prodrug system,[13] metal−carbonyl complexes are used as CORMs. The most common activation of CO release from these compounds in aqueous media is a solvent-mediated ligand exchange that starts immediately upon CORM administration,[3,4,7−10] but CO can also be liberated from CORMs via enzyme-triggered processes.[14−16]

Light-triggered CO liberation from a photochemically active CORM (photoCORM[17]) is an alternative activation strategy that allows for a precise spatial and temporal control over the CO release.[18] Transition metal-based complexes offer a relatively good flexibility and diversity in terms of their chemical composition and release efficiencies;[7,9,19] however, only a few such photoCORMs, for example, polypyridyl metallodendrimers,[20] Mn-complexes of azaheteroaromatic ligands,[21] or azopyridine,[22,23] absorb biologically benign visible light. CO release upon irradiation with 980 nm from a Mn-based nanocarrier via upconversion has also been recently shown.[24] Nevertheless, the design of new photoCORMs, which are chemically stable, nontoxic, and release CO efficiently upon visible light exposure, is still a major challenge.

PhotoCORMs based on organic compounds offer a great promise to address this challenge. Several examples of organic molecules, such as cyclopropenones,[25−28] 1,3-cyclobutanediones,[29] or 1,2-dioxolane-3,5-diones,[30] liberate CO upon biologically adverse UV or near-UV (<420 nm) light. To our knowledge, only two purely organic photoCORMs can be activated by visible light. Liao and co-workers have developed a system based on a cyclic aromatic α-diketone chromophore that liberates CO upon irradiation with light below ∼500 nm.[31] The molar absorption coefficients of such chromophores are however relatively low (only ∼1000 $dm^3\ mol^{-1}\ cm^{-1}$ at 458 nm[32]). Some of us have introduced a fluorescein analogue, 6-hydroxy-3-oxo-3*H*-xanthene-9-carboxylic acid (**1**; Scheme 1a), as a photoCORM that liberates CO along with the formation of 3,6-dihydroxy-9*H*-xanthen-9-one (**2**) upon irradiation below 520 nm in aqueous solutions at pH ≈ 7.[33] Although the CO-release quantum efficiency is low ($\Phi \approx 7 \times 10^{-4}$), the uncaging cross-section[18] evaluated as the product of Φ and the decadic molar absorption coefficient at the wavelength of irradiation (λ_{irr}), $\Phi\varepsilon$, is large (on the order of 1−10). Unfortunately, the synthesis of this compound is very difficult,[33] and we could not find an alternative pathway to produce it in sufficient quantities for further mechanistic studies that would allow us to modify

Received: June 26, 2015
Published: December 23, 2015

DOI: 10.1021/jacs.5b10800
J. Am. Chem. Soc. 2016, 138, 126−133

Scheme 1. (a) 6-Hydroxy-3-oxo-3*H*-xanthene-9-carboxylic Acid (1) as a PhotoCORM; and (b) Comparison of the Frontier MOs (Left, HOMO; Right, LUMO) of 6-Hydroxy-3-oxo-3*H*-xanthene (Top) and BODIPY (Bottom; Figure 1) Chromophores Using the Hückel MO Theory[a]

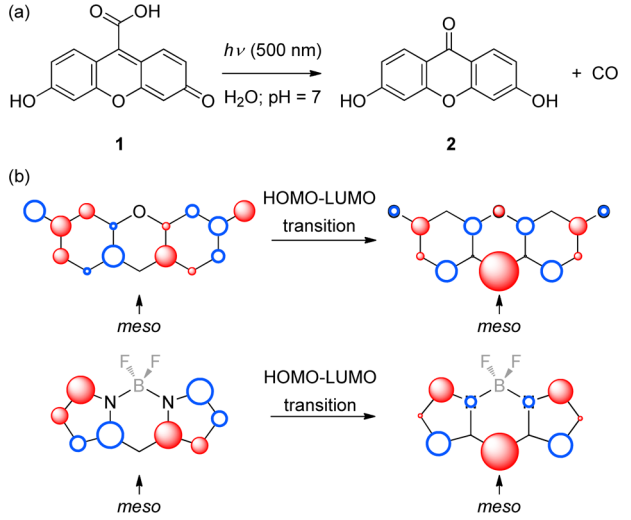

[a]The *meso* position in both chromophores is indicated by an arrow. The BF_2 group of BODIPY (in gray) was not explicitly considered in the Hückel calculation.

the chromophore properties and shift its absorption to longer wavelengths. We therefore decided to find an alternative chromophore that can be easily synthesized and exhibits photoreactivity similar to that of **1**.

Herein, we report the synthesis and properties of the *meso*-carboxy BODIPY (COR-BDP) derivatives **3a,b** (Figure 1) and

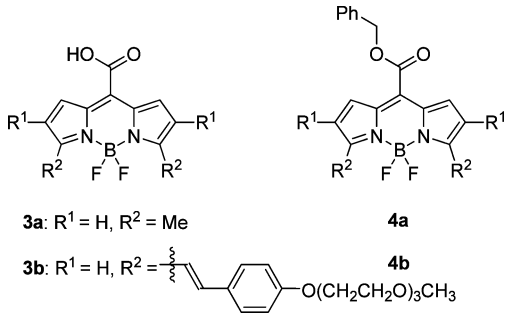

Figure 1. Structures of the BODIPY-based photoCORMs (COR-BDPs) **3a–c** and the synthetic precursors **4a,b**.

demonstrate their ability to efficiently release CO. We tested their bioavailability and potential toxicity in both in vitro and in vivo experimental settings, and we propose the mechanism of the CO release on the basis of steady-state and transient spectroscopy experiments and DFT calculations.

RESULTS AND DISCUSSION

In our previous work, we hypothesized that an α-lactone is formed in the *meso* position prior to the CO-release step upon irradiation of **1**.[33] Such an intermediate should be formed by a formal addition of the carboxylate oxygen to the *meso* position in an excited singlet or triplet state, possibly involving a photoinduced one-electron reduction step. Therefore, an alternative chromophore that preserves the photoreactivity of **1** should possess frontier molecular orbitals (MOs) with similar nodal properties at the *meso* position.[34]

Using Hückel molecular orbital (HMO) calculations, we screened the frontier molecular orbitals (MOs) of several well-known chromophores with strong absorption in the visible region, and we identified that the boron-dipyrromethene (BODIPY) molecule has a similar antisymmetric highest occupied MO (HOMO) as compared to that of **1** (Scheme 1b).[35] HMO predicts an increase in electronic density on the *meso* carbon atom upon the HOMO–LUMO excitation for both systems. Therefore, we deduced that *meso*-carboxy BODIPY derivatives (**3**, Figure 1) are promising photoCORM candidates. Many BODIPY derivatives have already received considerable attention in the past decade due to their distinctive and easily tunable optical properties.[36−38]

We first synthesized the model COR-BDP **3a** to evaluate its properties and ability to release CO. The preparation of a *meso*-carboxy BODIPY derivative analogous to **3a** has recently been reported.[39] The benzyl ester **4a** (Figure 1) was prepared as a synthetic precursor from benzyl chlorooxalate and 2-methylpyrrole.[40] This compound was then hydrogenated on Pd/C to obtain **3a** in 82% yield. Compound **3a** is soluble in aqueous solutions (>5 mM), and the pK_a of its carboxylic group in an aqueous solution, determined by potentiometric titration, was found to be (3.0 ± 0.2) (Figure S30). This value corresponds well with the pK_a's of coumarine-3-carboxylic acid[41] or xanthene-9-carboxylic acid (**1**).[33] Compound **3a** therefore exists as its conjugate base at physiological pH. Another protonation step occurs at a lower pH with $pK_a' = 1.69 \pm 0.02$ that affects the absorption properties of the chromophore (Figure S31). It is possible that a BF_2 moiety is displaced at such a low pH as observed in the case of other BODIPY derivatives.[42] The compound quickly decomposes at pH < 0.5. It is stable in the crystalline state (>3 weeks at room temperature) as well as in aqueous solutions (pH = 7.4, >2 weeks) in the dark. The absorption spectrum of an aqueous solution of **3a** (phosphate buffered saline, PBS; pH = 7.4; the ionic strength, I = 0.15 mol dm^{-3}) shows a major band with λ_{max} = 502 nm (Figure 2). The compound exhibits a bright fluorescence (Figure 2) with a quantum yield Φ_f of 67%. The corresponding excitation spectrum matches that of the absorption (Figure S17).

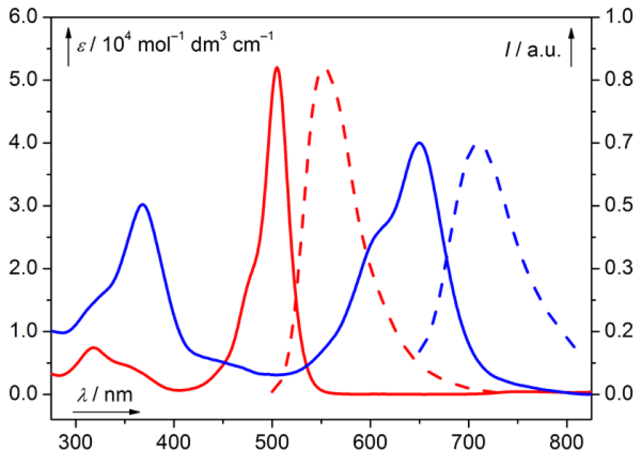

Figure 2. Absorption (solid lines) and normalized emission (dashed lines) spectra of **3a** (red) and **3b** (blue) (c = 1 × 10^{-5} mol dm^{-3}; phosphate buffered saline pH = 7.4; I = 0.15 mol dm^{-3}).

DOI: 10.1021/jacs.5b10800
J. Am. Chem. Soc. 2016, 138, 126–133

Compound **3a** underwent a complete decomposition upon irradiation at ~500 nm (Figure 3; top) with quantum yields of

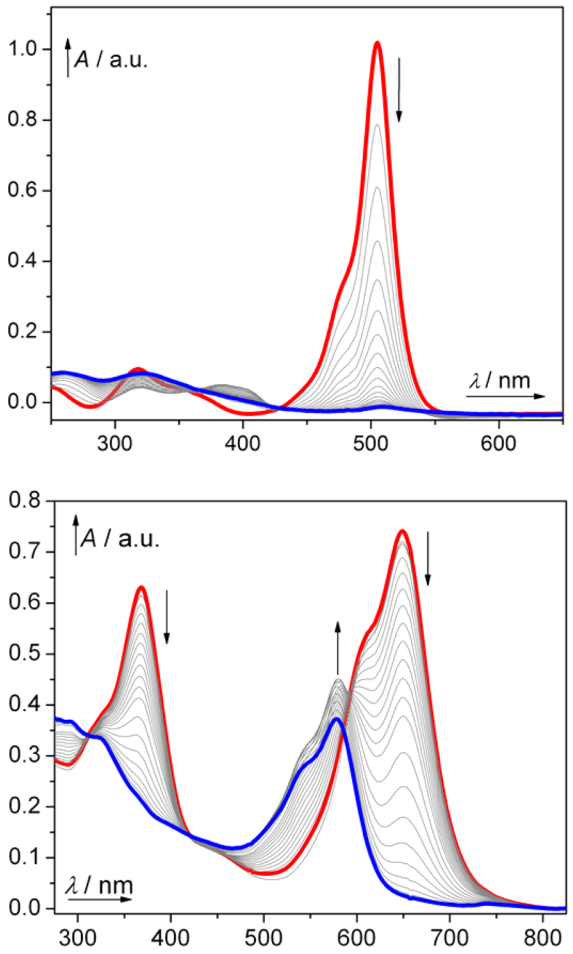

Figure 3. Irradiation of **3a** at 500 nm (top) and **3b** at 625 nm (bottom) in aerated phosphate buffer solutions (pH = 7.4). The spectra prior to (red line) and after (blue line) the irradiation are highlighted.

$(2.7 \pm 0.4) \times 10^{-4}$ and $(1.1 \pm 0.1) \times 10^{-4}$ in degassed and aerated PBS solutions (pH = 7.4), respectively (Table 1).[43] The product of $\Phi\varepsilon_{max}$ on the order of 10 is comparable to that of some of the common caged compounds, especially those absorbing near 400 nm.[18] The quantum yields were independent of the concentration of **3a** (Figures S27–S29).

Table 1. Photochemistry of 3a and 3b

compd[a]	Φ_{decomp}/%[b]	yield/%[c]	ε_{max}[d]	$\Phi\varepsilon_{max}$[e]
3a (deg)	$(2.7 \pm 0.4) \times 10^{-2}$	87	49 500	13
3a (aer)	$(1.1 \pm 0.1) \times 10^{-2}$	44		5
3b (deg)	$(1.2 \pm 0.4) \times 10^{-3}$	91	52 000	0.6
3b (aer)	$(1.4 \pm 0.4) \times 10^{-3}$	42		0.7

[a]In degassed (deg) or aerated (aer) phosphate buffer solutions (I = 0.1 M, pH = 7.4). [b]**1**[33] was used as an actinometer for **3a** and **3b**; ferrioxalate actinometer was also used for **3b**. Compounds **3a** and **3b** were irradiated at λ_{irr} = 505 and 365 nm (the second major absorption band), respectively. [c]The total maximum chemical yields of released CO, monitored by a GC/RGA headspace analysis, were obtained upon exhaustive irradiation. [d]The molar absorption coefficient, ε_{max}/(mol^{-1} dm^{-3} cm^{-1}). [e]The uncaging cross-section at λ_{max}.

Our GC/RGA analysis of CO released into the headspace of septum-sealed vials containing an irradiated sample evidenced that the decomposition of **3a** was accompanied by the formation of CO. Its total maximum chemical yield reached 87% upon complete conversion in the absence of oxygen (Table 1); that is, the quantum yield of decomposition corresponds reasonably to that of CO release. The maximum yield decreased to ~45% in aerated solutions, which was probably caused by bleaching of the starting material by the generated singlet oxygen (see later in the text). Only UV-light absorbing photoproducts were formed in the solution upon exhaustive irradiation. This is a great advantage as the photoproducts do not interfere with the photochemical process as internal filters.[18] HRMS analysis showed that the major products were 2-methylpyrrol and 2*H*-pyrrole-4-carbaldehyde (Figure S16) in accord with the reports that describe photochemical degradation of other BODIPY derivatives.[44] For comparison, the ester **4a** was irradiated under the same condition as **3a**. This compound was photochemically stable, and no CO release was detected. The carboxylic functional group is therefore essential for the reaction.

Encouraged with the results, we decided to design COR-BDP with a π-extended chromophore to shift the absorption to the phototherapeutic (or tissue-transparent) window (the region of 650–950 nm),[45] desired for biological and medical applications. There is currently no transition-metal-free caged compound that can be directly activated by light in this wavelength region. Only a few chemical systems releasing a chemical species upon irradiation with wavelengths above 450 but below ~600 nm are known,[18] for example, the (6-hydroxy-3-oxo-3*H*-xanthen-9-yl)methyl[33] or pyronin[46] derivatives introduced by our laboratory, 4-aryloxy BODIPY derivatives proposed by Urano and co-workers,[47] and the *meso*-methylhydroxy BODIPY scaffold designed simultaneously by the groups of Weinstain[48] and Winter.[49]

We synthesized COR-BDP **3b** by condensation of **4a** with the corresponding PEG-substituted benzaldehyde in the presence of piperidine in glacial acetic acid and subsequent hydrogenation on Pd/C in 56% yield. The 3,5-distyryl groups in **3b** affect the absorption properties of the BODIPY chromophore by extending the π-conjugation, whereas PEG chains enhance its aqueous solubility. The major absorption band of this compound (652 nm, tails to ~750 nm; Figure 2) is bathochromically shifted by ~150 nm as compared to that of **3a**. Excitation of **3b** at either of the main absorption bands (λ_{max} = 368 and 652 nm) resulted in the same fluorescence spectrum (Figure 2), that is, in the same emitting excited state. The presence of two styryl groups in **3b** is probably responsible for its lower fluorescence quantum yield (Φ_f = 12%) as compared to that of **3a** due to enhanced radiationless decay of the singlet excited state.[50,51]

Two protonation steps with pK_a' = (4.71 ± 0.01) and pK_a = (3.0 ± 0.2), respectively, have been identified; thus the conjugate base of **3b** is present at physiological pH (Figure S32). Irradiation of **3b** in an aqueous solution (PBS, pH = 7.4) released CO not only upon excitation at the major absorption band maxima (368 and 652 nm) but also at the absorption tail in the near-infrared region (732 nm). To our knowledge, COR-BDP **3b** is therefore the first caged compound that efficiently releases a molecule upon direct irradiation with near-infrared photons. Although the product of $\Phi\varepsilon$ decreases at longer wavelengths (see Table 1), it is still suitable for biological applications because the light penetrates deeply into the tissue.

DOI: 10.1021/jacs.5b10800
J. Am. Chem. Soc. 2016, 138, 126–133

This premise was confirmed by an in vivo experiment with a nude SKH1 mouse strain (Table 2). Hairless mice were used to facilitate light penetration through the cutaneous barrier. One group of mice that was not treated with **3b** served as a control group. Two other groups received intraperitoneal application of **3b** (50 μmol per kg of body weight). One group was left in the dark while the other was irradiated with white light focused to the abdominal area of mice for 4 h. Irradiation resulted in a substantial increase in both the carbonylhemoglobin (COHb) concentration in blood and the CO content in hepatic and kidney tissues, when compared to both nontreated and nonirradiated control groups. It should be noted that, although nonirradiated mice treated with **3b** were carefully kept in the dark, inadvertent light exposure of biological material (blood, liver), still containing unreacted **3b** during sampling, resulted in increased levels of COHb. Nevertheless, statistically unequivocal increase in the CO levels in both blood and tissues of irradiated mice as compared to both control groups (by factors of 1.5–2) clearly demonstrates that CO was photoreleased in vivo. Heme oxygenase induction, a possible source of CO overproduction, was excluded by a direct determination of heme oxygenase activity (Figure S49). In addition, an in vitro sample of blood containing **3b** was irradiated with white light, and the production of CO was detected by GC (Table S2).

Table 2. CO Release from 3b upon Irradiation in Vivo

group	w_{COHb}^{blood}/%[d]	c_{CO}^{liver}/pmol[e]	c_{CO}^{kidney}/pmol[f]
control[a]	0.36 ± 0.06	5.6 ± 1.2	7.1 ± 1.7
dark[b]	0.57 ± 0.04[g]	7.1 ± 1.1	7.0 ± 0.8
irradiated[c]	0.78 ± 0.18[g,h]	11.3 ± 2.7[g,h]	10.1 ± 0.8[g,h]

[a]A control group of 6 animals (no **3b** application). Another group of 12 animals received an intraperitoneal injection of **3b** in saline (50 μmol per kg of body weight), from which [b]6 mice were kept in the dark and [c]6 mice were irradiated with white light focused to the abdominal area. [d]w_{COHb}^{blood}: the relative amounts of COHb in the total amount of Hb in blood (in %); [e]c_{CO}^{liver} and [f]c_{CO}^{kidney}: the amounts of CO in pmol per 1 mg of a fresh liver and kidney tissue, respectively. The statistical significance: [g]*P*-value ≤0.05 vs "control group"; [h]*P*-value ≤0.05 vs "dark group"; n = 6 in each mice group.

The CO release from **3b** is accompanied by the concomitant formation of a yet-unidentified primary photoproduct that remains in the solution even after a prolonged photolysis (<10% conversion after 24 h) at wavelengths close to its absorption maximum (λ_{max} = 578 nm; Figure 3b). On the basis of the absorption spectrum, this compound still probably contains a BODIPY chromophore, but it does not represent an internal filter when the irradiation is conducted at wavelengths longer than the λ_{max} of **3b**. The decomposition quantum yields, the yields of CO release upon exhaustive irradiation, and the uncaging cross sections, $\Phi\varepsilon_{max}$, of **3b** when aerated or degassed samples were used are summarized in Table 1.

A controlled, steady, and long-lasting CO production is crucial for biological applications. Our GC/RGA analysis revealed a steady CO release for 100 and 26 h using **3a** and **3b**, respectively. The release rate depends on the intensity of the incident light. The formation of CO ceased when the irradiation was interrupted, allowing for complete control over the CO release (Figure 4).

Neither **3a**,**b** nor their photoproducts displayed toxicity[52] in our in vitro experiments on hepatoblastoma HepG2 and neuroblastoma SH-SY5Y cell lines up to concentrations of 100 μmol L^{-1} (Figure S39).

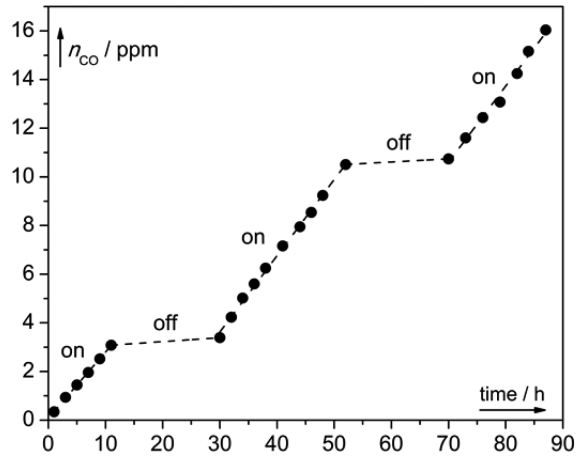

Figure 4. CO production from **3a**. **3a** (500 μM, PBS solution) was irradiated at 510 nm (11.6 mW cm^{-2}). The CO released to the vial headspace was measured by GC/RGA in 2–4 h intervals and expressed as the amount of CO (in ppm) released from **3a**. When irradiation (on) was interrupted (off), the vial was kept in the dark at 4 °C.

The influence of oxygen on the photolysis quantum yield of **3a** (Φ_{decomp} is lower by a factor of 2 in an aerated sample; Table 1) suggested that its triplet state might be involved in the CO release. However, intersystem crossing (isc) is not efficient in **3a** as evidenced by its high fluorescence quantum yield (Φ_f = 67%), which explains rather low decomposition quantum yields shown in Table 1. We thus synthesized a diiodo derivative **3c** (Figure 5; the synthesis and its photochemical properties are described in the Supporting Information) to enhance the isc rate via a heavy-atom effect as demonstrated on other BODIPY derivatives. For example, the isc quantum yield can reach 0.66 in a hexabromo-substituted BODIPY.[53] The absorption properties of **3c** are similar to those of **3a** (Figures 2 and S23); however, its fluorescence quantum yield dropped to Φ_f = 2% as expected. Unfortunately, the total chemical yield of released CO from **3c** was also very low (~3%). We concluded that the triplet excited **3c** undergoes a photoreaction that does not lead to the CO production (see the Supporting Information) either due to an alternative reaction pathway (i.e., a C–I bond fission) or due to bleaching by the generated singlet oxygen.

3c

Figure 5. A diiodo BODIPY derivative **3c**.

Nevertheless, laser flash spectroscopy of the compound **3c** helped us to assign the transient absorption signals of triplet **3a** that are of low intensity due to its inefficient isc. The transient triplet–triplet absorption spectrum of **3c** possesses three absorption maxima at 325, 415, and 660 nm (Figures S36–S38), which exhibit the same decay kinetics. Triplet-state absorption bands in the region of 410–450 nm have already been reported for analogous brominated BODIPY derivatives.[53] The lifetimes of the triplet **3c** under different conditions are shown in Table S1. The triplet state is markedly quenched by

DOI: 10.1021/jacs.5b10800
J. Am. Chem. Soc. 2016, 138, 126–133

oxygen; the lifetime of (34.5 ± 0.62) μs in a degassed aqueous buffer solution at pH = 7.4 dropped to (0.50 ± 0.02) μs in an oxygen-saturated sample. The triplet state of **3a** possesses absorption maxima at 430 and 640 nm with a lifetime of ∼(5 ± 1) μs in an aerated solution (Figure S35).

Final evidence that a triplet state is involved in the CO release was provided by irradiation of **3a** in a degassed aqueous solution containing CsCl (1 M aqueous solution; an analogous NaCl-containing sample was used as a reference) as a heavy-atom effect mediator[54] (Figure S34). We monitored the major absorption band of **3a** and observed that the decomposition quantum yield (Φ_{decomp}) increased by a factor of 1.6 in the presence of Cs^+ ions due to the isc-rate enhancement, while the fluorescence quantum yield decreased from 67% to 53%. The rate of the CO release monitored by a GC/RGA headspace analysis increased accordingly and matched that of **3a** decomposition.

This result motivated us to further explore the reaction mechanism. When a solution of **3a** was irradiated at pH = 2.5 where only 25% of **3a** exists in the form of the conjugate base, a decrease in Φ_{decomp} by a factor of ∼4 was observed (Figure S29). This suggests that the negative charge on the carboxyl group is essential for the reaction. The proton dissociation strongly influences the redox properties. For example, carboxylic acids have redox potentials, which are more positive than those of the corresponding carboxylates by ∼0.5 V.[55] The ground-state redox potential for **3a** was determined by cyclic voltammetry (−1.02 V vs SCE; the one-electron oxidation of **3a** (as a conjugate base) occurs at +0.13 V vs SCE; Figure S33). The former value corresponds well to the published data for other BODIPY derivatives.[56,57] The energy of the triplet excited state of a BODIPY could be estimated from the phosphorescence spectra of the dibromo (λ_{phos} = 740 nm, 1.68 eV)[58] or diiodo derivatives (λ_{phos} = 795 nm, 1.56 eV).[59] Using the latter value, the triplet state redox potential equals +0.54 V vs SCE. As a result, ΔG_{eT} of an intramolecular electron transfer between the carboxylate anion attached to an aromatic system and the triplet excited BODIPY moiety equals approximately −0.41 eV (−9.5 kcal mol^{-1}). In contrast, electron transfer between the protonated carboxylic acid and the BODIPY would be slightly endothermic (∼ +0.09 eV; +2 kcal mol^{-1}). Therefore, we hypothesized that an intramolecular photoinduced electron transfer (PET) takes place between the carboxylate and the BODIPY system in the triplet excited state.

This PET would result in the formation of a triplet diradical **5** (Scheme 2) with one electron on the carboxylate moiety and the other largely localized in the *meso* position of the BODIPY core (see HMOs in Scheme 1b). Such a structure resembles the oxyallyl diradical, the formation of which via photolysis of *p*-hydroxyphenacyl derivatives in aqueous solution was recently studied by some of us.[60] Its decay from a triplet to an open-shell singlet state is followed by the formation of a cyclopropanone intermediate that can be considered as a structural analogue of the anticipated α-lactone **6** (Scheme 2). It has already been reported that liberation of CO from α-lactones can occur in the dark.[61,62] In our previous study on 6-hydroxy-3-oxo-3*H*-xanthene-9-carboxylic acid (**1**),[33] the density functional theory (DFT) calculations failed to provide an evidence for the existence of the related α-lactone. We therefore decided to examine whether **6** may be formed prior to the CO release (Scheme 2). In this work, we attempted to find a potential energy minimum that would correspond to the structure of **6** on the singlet ground-state potential energy surface. By screening a series of well-performing functionals (see the Supporting Information for a detailed technical description), we found that the heterolysis of the α-lactone ring represents a difficult case to DFT methods. Thorough test calculations with a model smaller than but structurally similar to **6** (Supporting Information), which allowed the use of accurate perturbation and coupled-cluster methods, showed that the M06HF functional, which predicted that an energy minimum for **6** does exist, performs best of all of the DFT methods. We therefore conclude that the formation of **6** is feasible.

Scheme 2. Proposed Mechanism of COR-BDP Phototransformation To Release CO

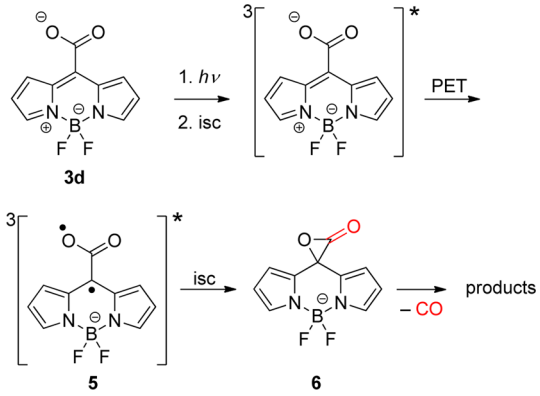

On the basis of our experimental and computational evidence, we propose the mechanism of CO release from COR-BDPs **3** (Scheme 2). Upon excitation, a strongly fluorescent, lowest excited singlet state of **3** undergoes relatively inefficient intersystem crossing to the triplet state where an exergonic PET from the carboxylate to the BODIPY chromophore takes place, resulting in the formation of an oxyallyl-type triplet diradical **5**. The subsequent intersystem crossing leads to the formation of α-lactone **6** on the singlet ground-state potential energy surface. Compound **6** then undergoes a nonphotochemical fragmentation to release CO.

■ CONCLUSIONS

We report a straightforward synthesis of a new generation of transition-metal-free CORMs based on BODIPY chromophores (COR-BDPs) that are activatable by visible-to-NIR (up to 730 nm) light. Such wavelengths are highly advantageous due to a better penetration of the light into biological tissues. We show the ability of COR-BDPs to efficiently release CO in a fully controllable way, and demonstrate their performance in both in vitro and in vivo experimental settings. The fluorescent nature of these chromophores could also be desirable for simultaneous in vivo imaging. We propose a mechanism of the CO release based on steady-state and transient absorption spectroscopy experiments and quantum chemical calculations. The BODIPY molecular scaffold allows for fine-tuning of the physicochemical properties of COR-BDPs (such as optical properties or aqueous solubility) using simple structural modification and promises a rapid development of improved CORM molecules. Further biological studies to prove the therapeutic potential of COR-BDPs are under investigation in our laboratories.

■ EXPERIMENTAL SECTION

Synthesis of 4a. Benzyl chlorooxalate (556 mg, 2.8 mmol) was added to a solution of 2-methylpyrrole (500 mg, 6.16 mmol) in

DOI: 10.1021/jacs.5b10800
J. Am. Chem. Soc. 2016, 138, 126−133

dichloromethane at 0 °C, and the mixture was stirred at 0 °C for 4 h. Triethylamine (1.96 mL, 14 mmol) was added, followed by an addition of $BF_3{\cdot}Et_2O$ (1.68 mL, 14 mmol). The solution was warmed to room temperature and stirred for 2 h. The reaction was quenched with aq HCl (10%), and the crude product was extracted with ethyl acetate. The organic layers were washed with water, dried with $MgSO_4$, filtered, and the solvents were evaporated to dryness. The compounds were purified by flash chromatography on silica gel using hexane/ethyl acetate (9:1) to give the pure compound **4a**. Yield: 110 mg (11%). Purple solid. Mp: >300 °C (decomp.). ^{1}H NMR (500 MHz, $CDCl_3$): δ (ppm) 7.48−7.40 (m, 5H, 5CH), 7.19 (d, J = 3.8 Hz, 2H, 2CH), 6.30 (d, J = 3.9 Hz, 2H, 2CH), 5.45 (s, 2H, CH_2), 2.64 (s, 6H, $2CH_3$) (Figure S1). ^{13}C NMR (125 MHz, $CDCl_3$): δ (ppm) 163.7 (C), 160.7 (C), 134.7 (C), 133.5 (C), 130.8 (CH), 128.8 (CH), 128.6 (CH), 128.0 (C), 120.7 (CH), 120.6 (CH), 68.2 (CH_2), 15.2 (CH_3) (Figure S2). FTIR (neat): 3065, 1725, 1567, 1458, 1374, 1163, 1101 cm^{-1}. HRMS (APCI): calcd for ($C_{19}H_{17}BF_2N_2O_2$) 353.1460, found 353.1459 (Figure S11).

Synthesis of 4b. 4-{2-[2-(2-Methoxyethoxy)ethoxy]ethoxy}-benzaldehyde (66 mg, 0.22 mmol), glacial acetic acid (0.08 mL, 1.8 mmol), piperidine (0.12 mL, 1.8 mmol), and a small amount of molecular sieves were added to a solution of **4a** (40 mg, 0.11 mmol) dissolved in anhydrous benzene (10 mL) in a round-bottomed flask equipped with a Dean−Stark head under argon atmosphere. The mixture was refluxed for 1 h. The solvent was then removed under reduced pressure, and the residue was diluted with ethyl acetate and washed with water. The organic layer was dried with $MgSO_4$, filtered, and concentrated under reduced pressure. The crude mixture was purified by flash chromatography on silica gel using hexane/dichloromethane (2:8) to give **4b**. Yield: 66 mg (70%). Green solid. Mp: >280 °C (decomp.). ^{1}H NMR (500 MHz, $CDCl_3$): δ (ppm) 7.55−7.49 (m, 6H, 6CH), 7.39−7.30 (m, 5H, 5CH), 7.25−7.22 (m, 4H, 4CH), 6.88 (d, J = 8.8 Hz, 4H, 4CH), 6.29 (d, J = 4.6 Hz, 2H, 2CH), 5.35 (s, 2H, CH_2), 4.11 (t, J = 4.8 Hz, 4H, 2-OCH_2), 3.82 (t, J = 4.9 Hz, 4H, OCH_2), 3.69−3.67 (m, 4H, OCH_2), 3.63−3.58 (m, 8H, OCH_2), 3.49−3.47 (m, 4H, OCH_2), 3.31 (s, 6H, OCH_3) (Figure S3). ^{13}C NMR (125 MHz, $CDCl_3$): δ (ppm) 164.2 (C), 160.2 (C), 156.5 (C), 138.1 (CH), 136.0 (C), 135.0 (C), 129.6 (CH), 129.5 (CH), 129.4 (CH), 128.8 (CH), 128.7 (CH), 128.6 (CH), 122.6 (C), 117.4 (CH), 115.1 (CH), 72.0 (CH_2), 70.9 (CH_2), 70.7 (CH_2), 70.6 (CH_2), 69.7 (CH_2), 67.6 (CH_2), 59.0 (CH_3) (Figure S4). FTIR (neat): 3085, 2920, 2851, 1717, 1593, 1349, 1158, 949 cm^{-1}. HRMS (ESI): calcd for ($C_{47}H_{53}BF_2N_2O_{10}$) 854.3761, found 854.3756 (Figure S12).

Synthesis of 3a. **4a** (50 mg, 014 mmol) was dissolved in dichloromethane (20 mL), and 10% Pd/C powder (5 mol %) was added under argon atmosphere, followed by addition of methanol (20 mL). The mixture was saturated with hydrogen and stirred at 25 °C for 2 h until no starting material remained. Pd/C was removed through filtration, and the solvent was evaporated under reduced pressure. The products were purified by flash chromatography using dichloromethane/methanol (8:2) on silica gel to give **3a**. Yield: 32 mg (82%). Yellow-orange solid. Mp: >250 °C (decomp.). ^{1}H NMR (500 MHz, D_2O): δ (ppm) 7.13 (d, J = 4.1 Hz, 2H, 2CH), 6.43 (d, J = 4.1 Hz, 2H, 2CH), 2.53 (s, 6H, $2CH_3$) (Figure S5). ^{13}C NMR (125 MHz, D_2O): δ (ppm) 170.5 (C), 158.6 (C), 139.0 (C), 131.2 (C), 129.7 (CH), 120.1 (CH), 14.2 (CH_3) (Figure S6). FTIR (neat): 3321, 3065, 1725, 1567, 1261, 1101, 1007, 945 cm^{-1}. HRMS (APCI): calcd for ($C_{12}H_{11}BF_2N_2O_2$) 262.0845, found 262.0844 (Figure S13).

Synthesis of 3b. **3b** was synthesized according to the same procedure as **3a** from **4c** (40 mg, 0.047 mmol). Yield: 19 mg (53%). Blue solid. Mp: >255 °C (decomp.). ^{1}H NMR (500 MHz, CD_3OD): δ (ppm) 7.62−7.57 (m, 6H, 6CH), 7.46 (d, J = 16.4 Hz, 2H, 2CH = CH), 7.28 (d, J = 4.4 Hz, 2H, 2CH), 7.06−7.02 (m, 6H, 6CH), 4.24 (t, J = 4.5 Hz, 4H, OCH_2), 3.89 (t, J = 4.6 Hz, 4H, OCH_2), 3.74−3.72 (m, 4H, OCH_2), 3.69−3.64 (m, 8H, OCH_2), 3.56−3.54 (m, 4H, OCH_2), 3.37 (s, 6H, OCH_3) (Figure S7). ^{13}C NMR (125 MHz, CD_3OD): δ (ppm) 169.6 (C), 159.9 (C), 154.6 (C), 135.7 (CH), 133.8 (C), 129.7 (C), 128.5 (CH), 116.9 (CH), 115.3 (CH), 114.8 (CH), 71.5 (CH_2), 70.4 (CH_2), 70.2 (CH_2), 70.0 (CH_2), 69.4 (CH_2), 67.4 (CH_2), 57.7 (CH_3) (Figure S8). FTIR (neat): 3331, 3075, 1721, 1575, 1302, 1132, 1007, 944 cm^{-1}. HRMS (ESI): calcd for ($C_{40}H_{47}BF_2N_2O_{10}$) 764.3292, found 764.3291 (Figure S14).

General Procedure for Irradiation in UV Cuvettes. A solution of a compound in the given solvent (3 mL) in a matched 1.0 cm quartz PTFE screw-cap cuvette equipped with a stir bar was stirred and irradiated with a light source of 32 LEDs emitting at the selected wavelength: λ_{max} = 365, 503, 525, 590, or 625 nm (the bandwidths at half height = 30 nm). Light pulses (425.6 Hz repetition rate, ≤150 fs pulse length, and energy of ∼7.5 ± 0.3 mW) from a Ti:Saphire laser coupled to a noncollinear optical parametric amplifier (NOPA) with the wavelength set to 505 nm (bandwidth at half height of ∼15 nm) were used to irradiate the samples. A 400 W broad-band halogen lamp with a filter (transmittance spectrum is shown in Figure S23) was used to irradiate the samples at 732 nm. The progress of reactions was monitored by UV−vis spectrometry using a diode-array spectrophotometer in a kinetic mode.

Quantum Yield Determination. The decomposition quantum yields of **3a** and **3b** were determined using a solution of xanthene-9-carboxylic acid (**1**, $c = 1.0 \times 10^{-5}$ M) in aq phosphate buffered saline (PBS, I = 0.1 M, pH = 7.4; $\Phi_{disapp.} = (6.8 \pm 3.0) \times 10^{-4}$)[33] as an actinometer and light pulses at 505 ± 7 nm (see above). The quantum yield of photodegradation of **3b** was determined at 365 nm with ferrioxalate actinometer[63] according to the published procedure.[64] The data were processed using a single value decomposition (SVD) software.

Determination of the Photoproducts. **3a** (500 mL, $c \approx 1 \times 10^{-5}$ M, aq solution) was irradiated in a large Petri dish (50 cm diameter) with a halogen lamp (500 W, Pyrex filter) for 38 h to reach a full conversion (the solution is photobleached). The resulting mixture was lyophilized to give the photoproducts, which were analyzed by HRMS (Figure S16).

Spectrophotometric Determination of pK_a's. A freshly prepared solution of **3a−c** ($c = 2.5 \times 10^{-5}$ M) in PBS (3 mL, I = 0.1 M, pH ≈ 7.4) was transferred into a matched 1.0 cm quartz cuvette, and its UV−vis absorption spectrum was recorded. The solution was acidified with HCl to pH ≈ 1 (10 μL of a 1 M solution) and was titrated with small additions of aq NaOH (typically 10 μL; 0.1, 0.01, or 0.001 M; I = 0.1 M, adjusted by NaCl), and the pH and UV−vis absorption spectra were monitored after each addition (Figures S31, S32).

Potentiometric Determination of pK_a's. A freshly prepared solution of **3a−c** ($c = 1 \times 10^{-3}$ M) in distilled water (5 mL) was stirred in a 25 mL beaker. The pH was measured potentiometrically, and the solution was acidified by HCl to pH ≈ 1 (10 μL, 1 M solution). The acidified solution was titrated with small additions of aq NaOH (typically 10 μL; 0.1, 0.01, or 0.001 M; I = 0.1 M, adjusted by NaCl), and the pH was measured after each addition. The volume of the added aq NaOH corresponding to every change in pH was recorded, and the titration curve was constructed (Figure S30).

Cyclic Voltammetry. Electrochemical studies were carried out with compounds dissolved in acetonitrile containing 0.1 M tetra-*n*-butylammonium hexafluorophosphate as a conducting salt using the ferrocene/ferrocenium (Fc/Fc^+) couple as an internal standard under argon atmosphere (Figure S33). The measurements were carried out in an optically transparent thin-layer electrochemical cell (0.1 mm optical length). A Pt minigrid working electrode, Pt minigrid reference electrode, and silver wire pseudoreference electrode were used. The measured potentials were recalculated to potentials vs SCE according to the published procedure.[65]

Determination of CO Concentrations. A solution of **3a−c** (0.25−2 mM) in PBS (20−150 μL, I = 0.1 M, pH ≈ 7.4) was added into CO-free septum-sealed glass vials. After irradiation with white light (433 mW cm^{-2}; 10 cm from the light source) or 510 ± 5 nm (11.6 mW cm^{-2}; Edmund Optics Barrington filter No. 65152), the CO amount released into the vial headspace was determined by gas chromatography with a reduction gas analyzer described previously.[66]

In Vitro Toxicity Determination. Human neuroblastoma SHSY5Y and hepatoblastoma HepG2 cell lines were grown according to the manufacturer's protocol in a 96-well plate with solutions of **3a** and **3b** or their photoproducts in the concentration range of 10−100

DOI: 10.1021/jacs.5b10800
J. Am. Chem. Soc. 2016, 138, 126−133

μM for 4, 24, or 48 h. The viability of cell lines was determined by a 3-(4,5-dimethylthiazol-2-yl)-2,5-diphenyltetrazolium bromide assay (MTT). After 2 h incubation period with MTT, the absorbance of a formazan-reduction product was measured at 545 nm with a standard ELISA reader. Compounds **3a** and **3b** were found not to interfere with the reduction of MTT.

In Vivo Experiments. Male nude SKH1 mice were allowed water and standard granulated diet ad libitum. All studies in this work met the criteria for the care and use of animals, and were approved by the Animal Research Committee of the 1st Faculty of Medicine, Charles University in Prague. Mice were anesthetized and then received an intraperitoneal injection of saline (a control group) or a solution of **3b** in saline (50 μmol per 1 kg of body weight). An experimental group of mice was irradiated with a lamp focused to the abdominal area for 4 h, while a control group was kept in the dark. Subsequently, the animals were sacrificed. Blood from the superior vena cava of each animal was transferred to the test tubes containing aq solution of EDTA (2 μL; 0.5 M). The CO (as COHb) and total hemoglobin concentrations in the sample of blood (1 μL) were determined using GC and a Drabkin cyanmethemoglobin method described previously.[67] Liver and kidneys of each animal were then harvested, washed, put into an ice-cold potassium phosphate buffer (c = 0.1 M, pH = 7.4) in a ratio of 1:4 (w/w), and homogenized by sonication. The liver/kidneys homogenate (40 μL) was added to CO-free septum-sealed vials containing 5 μL of 60% (v/w) sulfosalicylic acid. After incubation on ice (30 min), the amount of the CO released into the vial headspace was determined by GC/RGA as reported previously.[68]

Statistical Analyses. The data from in vivo experiments are expressed as mean ± standard deviations. The Student's t test was used to determine the significance of the differences among the study mice groups. The resulting P-values ≤0.05 (Table 2) were considered as statistically significant.

Quantum Chemical Calculations. The Hückel molecular orbital theory calculations were done with a freeware program HULIS.[69,70] The structure of the BODIPY chromophore was approximated with dipyrrin because the Hückel theory applies only to π-systems. The density functional theory (DFT) and ab initio calculations were performed with the Gaussian 09 package[71] of electronic structure programs. Gas-phase constrained geometry optimizations to compute the potential energy surfaces along the *meso*-carbon of BODIPY and the oxygen of α-lactone bond length were performed with a series of DFT (B3LYP, CAM-B3LYP, BMK, M06HF, M06-2X, and ωB97X) and perturbation theory (MP2 and MP4(SDQ)) methods with a 6-311+G(d) basis set. Full geometry optimization was performed with selected DFT methods with 6-31G(d) or 6-311+G(d) basis sets using the polarizable continuum model (PCM) as implemented in Gaussian to mimic the solvation effects (acetonitrile or water) or the gas phase. Harmonic vibrational frequencies were computed for the stationary points. Single point energies on the geometries obtained by the constrained geometry optimization at the MP4(SDQ)/6-311+G(d) or M06HF/6-311+G(d) level of theory were computed by MP4(SDTQ), QCISD(T), and CCSD(T) ab initio methods with the use of a cc-pVTZ basis set.

■ ASSOCIATED CONTENT

Supporting Information

The Supporting Information is available free of charge on the ACS Publications website at DOI: 10.1021/jacs.5b10800.

Materials and methods; synthesis and photochemistry of **3c**; steady-state spectroscopy results; potentiometry data; laser flash spectroscopy results; lifetime measurements; toxicity and heme oxygenase activity measurements; details of quantum chemical calculations; and additional characterization data (PDF).

■ AUTHOR INFORMATION

Corresponding Author

*klan@sci.muni.cz

Author Contributions

‖E.P. and T.S. contributed equally to this work.

Notes

The authors declare no competing financial interest.

■ ACKNOWLEDGMENTS

Support for this work was provided by the Czech Science Foundation (GA13-25775S) (P.K.) and Czech Ministry of Health (RVO-VFN64165/2015) (L.V.). The RECETOX research infrastructure was supported by the projects of the Czech Ministry of Education (LO1214 and LM2011028). We also thank Marie Zadinová and Jakub Šuk for their technical assistance with in vivo experiments, Jana Vaníková for performing MTT assays, Kateřina Klánová for her help with TOC, and Jakob Wirz for fruitful discussions.

■ REFERENCES

(1) Boczkowski, J.; Poderoso, J. J.; Motterlini, R. *Trends Biochem. Sci.* **2006**, *31*, 614−621.
(2) Motterlini, R.; Otterbein, L. E. *Nat. Rev. Drug Discovery* **2010**, *9*, 728−743.
(3) Romao, C. C.; Blattler, W. A.; Seixas, J. D.; Bernardes, G. J. L. *Chem. Soc. Rev.* **2012**, *41*, 3571−3583.
(4) Garcia-Gallego, S.; Bernardes, G. J. L. *Angew. Chem., Int. Ed.* **2014**, *53*, 9712−9721.
(5) Ahmad, S.; Hewett, P. W.; Fujisawa, T.; Sissaoui, S.; Cai, M.; Gueron, G.; Al-Ani, B.; Cudmore, M.; Ahmed, S. F.; Wong, M. K. K.; Wegiel, B.; Otterbein, L. E.; Vitek, L.; Ramma, W.; Wang, K. Q.; Ahmed, A. *Thromb. Haemostasis* **2015**, *113*, 329−337.
(6) Vitek, L.; Gbelcova, H.; Muchova, L.; Vanova, K.; Zelenka, J.; Konickova, R.; Suk, J.; Zadinova, M.; Knejzlik, Z.; Ahmad, S.; Fujisawa, T.; Ahmed, A.; Ruml, T. *Dig. Liver Dis.* **2014**, *46*, 369−375.
(7) Schatzschneider, U. *Br. J. Pharmacol.* **2015**, *172*, 1638−1650.
(8) Heinemann, S. H.; Hoshi, T.; Westerhausen, M.; Schiller, A. *Chem. Commun.* **2014**, *50*, 3644−3660.
(9) Schatzschneider, U. *Eur. J. Inorg. Chem.* **2010**, *2010*, 1451−1467.
(10) Mann, B. E. *Organometallics* **2012**, *31*, 5728−5735.
(11) Motterlini, R.; Mann, B. E.; Foresti, R. *Expert Opin. Invest. Drugs* **2005**, *14*, 1305−1318.
(12) Motterlini, R.; Sawle, P.; Hammad, J.; Bains, S.; Alberto, R.; Foresti, R.; Green, C. J. *FASEB J.* **2005**, *19*, 284−286.
(13) Wang, D. Z.; Viennois, E.; Ji, K.; Damera, K.; Draganov, A.; Zheng, Y. Q.; Dai, C. F.; Merlin, D.; Wang, B. H. *Chem. Commun.* **2014**, *50*, 15890−15893.
(14) Romanski, S.; Kraus, B.; Guttentag, M.; Schlundt, W.; Rucker, H.; Adler, A.; Neudorfl, J.-M.; Alberto, R.; Amslinger, S.; Schmalz, H.-G. *Dalton T.* **2012**, *41*, 13862−13875.
(15) Romanski, S.; Kraus, B.; Schatzschneider, U.; Neudörfl, J.-M.; Amslinger, S.; Schmalz, H.-G. *Angew. Chem., Int. Ed.* **2011**, *50*, 2392−2396.
(16) Sitnikov, N. S.; Li, Y.; Zhang, D.; Yard, B.; Schmalz, H.-G. *Angew. Chem., Int. Ed.* **2015**, *54*, 12314−12318.
(17) Rimmer, R. D.; Richter, H.; Ford, P. C. *Inorg. Chem.* **2010**, *49*, 1180−1185.
(18) Klan, P.; Solomek, T.; Bochet, C. G.; Blanc, A.; Givens, R.; Rubina, M.; Popik, V.; Kostikov, A.; Wirz, J. *Chem. Rev.* **2013**, *113*, 119−191.
(19) Schatzschneider, U. *Inorg. Chim. Acta* **2011**, *374*, 19−23.
(20) Govender, P.; Pai, S.; Schatzschneider, U.; Smith, G. S. *Inorg. Chem.* **2013**, *52*, 5470−5478.
(21) Gonzalez, M. A.; Carrington, S. J.; Fry, N. L.; Martinez, J. L.; Mascharak, P. K. *Inorg. Chem.* **2012**, *51*, 11930−11940.

DOI: 10.1021/jacs.5b10800
J. Am. Chem. Soc. 2016, 138, 126−133

(22) Carrington, S. J.; Chakraborty, I.; Mascharak, P. K. *Chem. Commun.* **2013**, *49*, 11254−11256.
(23) Chakraborty, I.; Carrington, S. J.; Mascharak, P. K. *Acc. Chem. Res.* **2014**, *47*, 2603−2611.
(24) Pierri, A. E.; Huang, P. J.; Garcia, J. V.; Stanfill, J. G.; Chui, M.; Wu, G.; Zheng, N.; Ford, P. C. *Chem. Commun.* **2015**, *51*, 2072−2075.
(25) Kuzmanich, G.; Gard, M. N.; Garcia-Garibay, M. A. *J. Am. Chem. Soc.* **2009**, *131*, 11606−11614.
(26) Poloukhtine, A.; Popik, V. V. *J. Org. Chem.* **2003**, *68*, 7833−7840.
(27) Poloukhtine, A.; Popik, V. V. *J. Phys. Chem. A* **2006**, *110*, 1749−1757.
(28) Poloukhtine, A. A.; Mbua, N. E.; Wolfert, M. A.; Boons, G.-J.; Popik, V. V. *J. Am. Chem. Soc.* **2009**, *131*, 15769−15776.
(29) Kuzmanich, G.; Garcia-Garibay, M. A. *J. Phys. Org. Chem.* **2011**, *24*, 883−888.
(30) Chapman, O. L.; Wojtkowski, P. W.; Adam, W.; Rodriguez, O.; Rucktaeschel, R. *J. Am. Chem. Soc.* **1972**, *94*, 1365−1367.
(31) Peng, P.; Wang, C. M.; Shi, Z.; Johns, V. K.; Ma, L. Y.; Oyer, J.; Copik, A.; Igarashi, R.; Liao, Y. *Org. Biomol. Chem.* **2013**, *11*, 6671−6674.
(32) Birnbaum, H.; Cookson, R. C.; Lewin, N. *J. Chem. Soc.* **1961**, 1224−&.
(33) Antony, L. A. P.; Slanina, T.; Sebej, P.; Solomek, T.; Klan, P. *Org. Lett.* **2013**, *15*, 4552−4555.
(34) Similar nodal properties of frontier MOs is a necessary but not sufficient condition for predicting the same type of photoreaction of two, seemingly unrelated chromophores.
(35) Šolomek, T.; Wirz, J.; Klán, P. *Acc. Chem. Res.* **2015**, DOI: 10.1021/acs.accounts.5b00400.
(36) Boens, N.; Leen, V.; Dehaen, W. *Chem. Soc. Rev.* **2012**, *41*, 1130−1172.
(37) Bessette, A.; Hanan, G. S. *Chem. Soc. Rev.* **2014**, *43*, 3342−3405.
(38) Lu, H.; Mack, J.; Yang, Y. C.; Shen, Z. *Chem. Soc. Rev.* **2014**, *43*, 4778−4823.
(39) Ni, Y.; Zeng, L. T.; Kang, N. Y.; Huang, K. W.; Wang, L.; Zeng, Z. B.; Chang, Y. T.; Wu, J. S. *Chem. - Eur. J.* **2014**, *20*, 2301−2310.
(40) Lo, M. M. C.; Fu, G. C. *J. Am. Chem. Soc.* **2002**, *124*, 4572−4573.
(41) Varlan, A.; Hillebrand, M. *Cent. Eur. J. Chem.* **2011**, *9*, 624−634.
(42) Yu, M. F.; Wong, J. K. H.; Tang, C.; Turner, P.; Todd, M. H.; Rutledge, P. J. *Beilstein J. Org. Chem.* **2015**, *11*, 1−5.
(43) The benzyl ester **4a** is stable upon irradiation in both degassed and aerated methanolic solutions (Figure S29).
(44) Mula, S.; Ray, A. K.; Banerjee, M.; Chaudhuri, T.; Dasgupta, K.; Chattopadhyay, S. *J. Org. Chem.* **2008**, *73*, 2146−2154.
(45) Konig, K. *J. Microsc.* **2000**, *200*, 83−104.
(46) Stacko, P.; Sebej, P.; Veetil, A. T.; Klán, P. *Org. Lett.* **2012**, *14*, 4918−4921.
(47) Umeda, N.; Takahashi, H.; Kamiya, M.; Ueno, T.; Komatsu, T.; Terai, T.; Hanaoka, K.; Nagano, T.; Urano, Y. *ACS Chem. Biol.* **2014**, *9*, 2242−2246.
(48) Rubinstein, N.; Liu, P.; Miller, E. W.; Weinstain, R. *Chem. Commun.* **2015**, *51*, 6369−6372.
(49) Goswami, P. P.; Syed, A.; Beck, C. L.; Albright, T. R.; Mahoney, K. M.; Unash, R.; Smith, E. A.; Winter, A. H. *J. Am. Chem. Soc.* **2015**, *137*, 3783−3786.
(50) Ortiz, M. J.; Garcia-Moreno, I.; Agarrabeitia, A. R.; Duran-Sampedro, G.; Costela, A.; Sastre, R.; Arbeloa, F. L.; Prieto, J. B.; Arbeloa, I. L. *Phys. Chem. Chem. Phys.* **2010**, *12*, 7804−7811.
(51) Costela, A.; Garcia-Moreno, I.; Pintado-Sierra, M.; Amat-Guerri, F.; Liras, M.; Sastre, R.; Arbeloa, F. L.; Prieto, J. B.; Arbeloa, I. L. *J. Photochem. Photobiol., A* **2008**, *198*, 192−199.
(52) Kostova, I. *Curr. Med. Chem.* **2006**, *13*, 1085−1107.
(53) Zhang, X. F.; Yang, X. D. *J. Phys. Chem. B* **2013**, *117*, 5533−5539.
(54) Saito, F.; Tobita, S.; Shizuka, H. *J. Chem. Soc., Faraday Trans.* **1996**, *92*, 4177−4185.
(55) Perkins, R. J.; Xu, H. C.; Campbell, J. M.; Moeller, K. D. *Beilstein J. Org. Chem.* **2013**, *9*, 1630−1636.
(56) Palao, E.; Agarrabeitia, A. R.; Banuelos-Prieto, J.; Lopez, T. A.; Lopez-Arbeloa, I.; Armesto, D.; Ortiz, M. J. *Org. Lett.* **2013**, *15*, 4454−4457.
(57) Nepomnyashchii, A. B.; Bard, A. J. *Acc. Chem. Res.* **2012**, *45*, 1844−1853.
(58) Banerjee, S.; Kuznetsova, R. T.; Papkovsky, D. B. *Sens. Actuators, B* **2015**, *212*, 229−234.
(59) Zhang, X. F.; Yang, X. D.; Niu, K.; Geng, H. *J. Photochem. Photobiol., A* **2014**, *285*, 16−20.
(60) Solomek, T.; Heger, D.; Ngoy, B. P.; Givens, R. S.; Klan, P. *J. Am. Chem. Soc.* **2013**, *135*, 15209−15215.
(61) Labbe, G. *Angew. Chem., Int. Ed. Engl.* **1980**, *19*, 276−289.
(62) Showalter, B. M.; Toscano, J. R. *J. Phys. Org. Chem.* **2004**, *17*, 743−748.
(63) Hatchard, C. G.; Parker, C. A. *Proc. R. Soc. London, Ser. A* **1956**, *235*, 518−536.
(64) Klan, P.; Wirz, J. *Photochemistry of Organic Compounds: From Concepts to Practice*, 1st ed.; John Wiley & Sons Ltd.: Chichester, 2009.
(65) Pavlishchuk, V. V.; Addison, A. W. *Inorg. Chim. Acta* **2000**, *298*, 97−102.
(66) Vreman, H. J.; Stevenson, D. K. *Anal. Biochem.* **1988**, *168*, 31−38.
(67) Vreman, H. J.; Kwong, L. K.; Stevenson, D. K. *Clin. Chem.* **1984**, *30*, 1382−1386.
(68) Vreman, H. J.; Wong, R. J.; Kadotani, T.; Stevenson, D. K. *Anal. Biochem.* **2005**, *341*, 280−289.
(69) Hagebaum-Reignier, D.; Girardi, R.; Carissan, Y.; Humbel, S. *J. Mol. Struct.: THEOCHEM* **2007**, *817*, 99−109.
(70) Carissan, Y.; Hagebaum-Reignier, D.; Goudard, N.; Humbel, S. *J. Phys. Chem. A* **2008**, *112*, 13256−13262.
(71) Frisch, M. J.; Trucks, G. W.; Schlegel, H. B.; Scuseria, G. E.; Robb, M. A.; Cheeseman, J. R.; Scalmani, G.; Barone, V.; Mennucci, B.; Petersson, G. A.; Nakatsuji, H.; Caricato, M. L.; Hratchian, H. P. I.; Bloino, J.; Zheng, G.; Sonnenberg, J. L.; Hada, M.; Ehara, M.; Toyota, K.; Fukuda, R.; Hasegawa, J. I.; Nakajima, T.; Honda, Y.; Kitao, O.; Nakai, H.; Vreven, T.; Montgomery, J. A., Jr.; Peralta, J. E.; Ogliaro, F.; Bearpark, M.; Heyd, J. J.; Brothers, E.; Kudin, K. N.; Staroverov, V. N.; Kobayashi, R.; Normand, J.; Raghavachari, K.; Rendell, A.; Burant, J. C.; Iyengar, S. S.; Tomasi, J.; Cossi, M.; Rega, N.; Millam, J. M.; Klene, M.; Knox, J. E.; Cross, J. B.; Bakken, V.; Adamo, C.; Jaramillo, J.; Gomperts, R.; Stratmann, R. E.; Yazyev, O.; Austin, A. J. C.; Pomelli, C.; Ochterski, J. W.; Martin, R. L.; Morokuma, K.; Zakrzewski, V. G.; Voth, G. A.; Salvador, P.; Dannenberg, J. J.; Dapprich, S.; Daniels, A. D.; Farkas, O.; Foresman, J. B.; Ortiz, J. V.; Cioslowski, J.; Fox, D. J. *Gaussian 09*; Gaussian, Inc.: Wallingford, CT, 2009.

DOI: 10.1021/jacs.5b10800
J. Am. Chem. Soc. 2016, 138, 126−133